Applied Catalysis B: Environmental 111–112 (2012) 81–89

Contents lists available at SciVerse ScienceDirect

Applied Catalysis B: Environmental

journal homepage: www.elsevier.com/locate/apcatb

Supported gold nanoparticle catalysts for wet peroxide oxidation

A. Quintanilla [a,*], S. García-Rodríguez [b], C.M. Domínguez [a], S. Blasco [a], J.A. Casas [a], J.J. Rodriguez [a]

[a] Area de Ingeniería Química, Universidad Autónoma de Madrid, Campus de Cantoblanco, 28049, Madrid, Spain
[b] Departamento de Estructura y Reactividad de Catalizadores, Instituto de Catálisis y Petroleoquímica (CSIC), C/Marie Curie 2, 28049 Madrid, Spain

ARTICLE INFO

Article history:
Received 17 May 2011
Received in revised form 8 September 2011
Accepted 19 September 2011
Available online 24 September 2011

Keywords:
Gold
Nanoparticle
Hydrogen peroxide
Catalytic wet oxidation
Oxidation pathway

ABSTRACT

Supported gold nanoparticles are of promising interest in wet hydrogen peroxide oxidation processes due to their efficient hydrogen peroxide consumption and adequate stability. Here, the origin of the catalytic properties of gold in this environmental process is explored by analyzing the influence of the support and the particle size on the activity of supported gold nanoparticles along with the influence of the nature of the target pollutant on the gold reactivity. The reaction mechanism for the oxidation of phenol with activated carbon-supported gold nanoparticles is proposed and the selectivity evaluated. A reaction pathway has been also proposed.

The results demonstrate that wet peroxide oxidation is a support and gold size dependent reaction. Activated carbon is the preferable candidate *versus* TiO_2 and Fe_2O_3 supports and small gold nanoparticles, desirably lower than 3 nm, show the highest TOF values. Supports showing adsorption capacity towards the target pollutant contribute to a more efficient use of hydrogen peroxide and, improve the TOF values for the oxidation and mineralization. Organic pollutants forming intermediate complexes with gold, *viz.* alcohols, are more efficiently oxidized. The inclusion of gold improves substantially the selectivity towards mineralization with respect to the bare activated carbon.

1. Introduction

The catalytic wet peroxide oxidation (CWPO) process relies on the oxidation of suspended or diluted organic matter in water under mild operating conditions (T = 298–383 K, P = 1–5 atm) using hydrogen peroxide as oxidant. The main active species for the oxidation is the hydroxyl radical, produced from hydrogen peroxide decomposition catalyzed by iron. The system $H_2O_2 + Fe^{2+}$ is the well-known Fenton reagent [1,2]. The current commercial units (US Peroxide, OXY-PURE®, OHP® and PROX T.E.C) are based on this catalytic system because of the operational simplicity and low-cost in comparison with other advanced oxidation processes [3]. However, it also presents several drawbacks derived from the operating pH (which must be maintained around 3, [4]), loss of iron with the consequent production of iron waste sludge and catalytic inhibition upon iron sequestering by-some of the reaction by-products giving rise iron-organic complexes [5,6]. These problems can be diminished by the immobilization of the iron on a support, *i.e.* alumina [7,8], silica [9,10], mesoporous silica [11–15], pillared clays [16–20], zeolites [21–25], activated carbon [26–29], carbon aerogels [30,31] and carbon nanotubes [32].

Unfortunately, these iron-heterogeneous systems show other different drawbacks derived from the low-efficient consumption of hydrogen peroxide, since some supports such as activated carbons can contribute to the inefficient decomposition of hydrogen peroxide into oxygen [33]. The poor stability of the catalysts, caused by iron leaching, is also a matter of concern [4,5,10,27,28,14]. In this sense, gold has recently shown its supremacy. The novel work of Han et al. [34], presented gold as active catalysts in wet peroxide oxidation processes, demonstrating the superior stability of gold-on-hydroxyapatite over Fe/ZSM-5 catalyst in the treatment of low-polluted wastewater (*i.e.* 0.1 g/L organic contaminant such as phenol). Later, Quintanilla et al. [35], demonstrated the use of gold catalysts also for medium-loaded wastewater (*i.e.* 1–5 g/L phenol). In that work, the presence of hydroxyl radicals was proved, by using a selective quencher, and a reaction mechanism was proposed based on the redox cycle accomplished between Au^0 and Au^+ species:

$$Au^0 + H_2O_2 \rightarrow HO^\bullet + HO^- + Au^+ \quad (1)$$

$$Au^+ + H_2O_2 \rightarrow {}^\bullet OOH + H^+ + Au^0 \quad (2)$$

Recently, the work of Martín et al. [36], working with gold-on-nanosized diamond prepared in a previous work [37], demonstrated that small gold nanoparticles (sizes lower than 1 nm) supported on diamond nanoparticles are an efficient catalyst in the sense of achieving adequate biodegradability of phenolic wastewater with values of H_2O_2 to phenol molar ratio as low as 4, which is

* Corresponding author. Tel.: +34 914972878; fax: +34 914973516.
E-mail address: asun.quintanilla@uam.es (A. Quintanilla).

0926-3373/$ – see front matter © 2011 Elsevier B.V. All rights reserved.
doi:10.1016/j.apcatb.2011.09.020

6.5 times lower than the theoretical stoichiometric amount of H_2O_2 usually employed for complete phenol oxidation (mineralization).

Herein, an insight into the origin of the catalytic properties of gold in wet peroxide oxidation is accomplished. The influence of the nature of the support and the size of gold particles deposited on a support have been explored along with the effect of the nature of the pollutant on the gold reactivity. Experimental work on small gold particles immobilized on different supports (TiO_2, C and Fe_2O_3) used in the oxidation of two different target compounds (*viz.* phenol and benzyl alcohol) has been performed along with an study of the catalytic behavior of size-selected gold particles deposited on activated carbon in the wet peroxidation of phenol. The results have been analyzed in terms of conversions, initial rates and Turn-over-Frequencies (TOFs) and supported with TEM and XPS analyzes. The reaction mechanism for the oxidation of phenol with activated carbon-supported gold nanoparticles is proposed and the selectivity evaluated. A reaction pathway has been also proposed.

2. Experimental

2.1. Catalysts

0.8 wt%·Au/TiO_2 (Mintek, batch: BC14) and 4.5 wt%·Au/Fe_2O_3 (Word Gold Council) catalysts were used as-received. In addition, size-selected Au/C catalysts (C is an activated carbon supplied by Merck, Ref.: 102514, S_{BET} = 973 m^2/g, A_{ext} = 175 m^2/g, V_{micro} = 0.38 cm^3/g) were prepared in our lab by the gold-sol immobilization method. Different aqueous gold colloids were used: 3 nm citrate-capped gold (Strem Chemicals Inc.) and 5.1 ± 0.7, 7.2 ± 0.5 and 9.8 ± 1.4 nm tannic acid-capped gold nanoparticles (Nanocomposix). The appropriate volume of the spherical-shape particles suspension was stirred overnight with the corresponding mass of carbon in order to obtain the targeted content of gold of 0.5 wt%. The red colour of the colloid solution faded overnight indicating the removal of gold from the aqueous phase; carbon did not apparently change in colour. After stirring, the suspension was dried at 333 K until complete evaporation of the remaining solution. The resulting Au/C catalyst was subsequently washed with water and dried. The catalysts are designated as Au(3)/C, Au(5)/C, Au(7)/C and Au(10)/C according to the original average size (nm) of gold in the colloid.

The gold content of the catalysts was determined by ICP (Elan 6000 PerkinElmer Sciex) and confirmed by fluorescence spectroscopy (Si–Li detector in a TXRF Extra-II Rich & Seifert spectrometer). The gold particle size distribution was obtained with a 200 kV JEM-2100F transmission electron microscope (JEOL Ltd.) by observation of several micrographs taken from different regions of the particular catalysts. In the case of Au/TiO_2 catalyst, small crystalline gold particles were not clearly distinguished from crystalline TiO_2. Then, the observation of this sample was performed in scanning mode and recorded with an annular dark field detector with an inner detection angle of 68.5 mrad (HAADF-STEM). The contrast in this mode is a function of atomic number, which enabled the straight gold particle observation.

The exposed gold surface species (Au^0, $Au^{\delta+}$) were quantified by XPS. Spectra were recorded using a VG Escalab 200R electron spectroscope equipped with a hemispherical analyzer, operating in a constant pass energy mode and a non-monochromatic Mg Kα ($h\nu$ = 1253.6 eV, 1 eV = 1.603×10^{-19} J). X-ray source operated at 10 mA and 12 kV. The energy regions of the photoelectrons of interest were scanned a number of times in order to get good signal-to-noise ratios. The intensities of the peaks were estimated by calculating the integral of each peak after subtracting a Shirley type background and fitting the experimental peak to a combination of Lorenzian/Gaussian lines of variable proportions. The binding energies (BE) were referenced to the C1s peak (284.6 eV).

2.2. Wet peroxide oxidation experiments

The oxidation tests were carried out batch-wise in a magnetically stirred three-necked glass reactor equipped with a reflux condenser. In a typical experiment, 45 mL of distilled water containing 5 g/L of phenol or benzyl alcohol (Sigma–Aldrich) at pH 3.5 (HCl, Sigma–Aldrich) was placed in the flask, along with 0.125 g of catalyst. This acidic pH was selected in order to work within the range of pH values used in heterogeneous Fenton process, in which some leaching of Fe is usually observed. Then, the reaction content was heated to 353 K (IKA RCT basic). Once this temperature was reached, 5 mL of an adjusted concentration of hydrogen peroxide (Sigma–Aldrich) was injected and the stirring at 1200 rpm started. After 24 h of reaction, the heating and stirring were switched-off and the flask cooled to room temperature by soaking in a crushed ice bath. Then the catalyst was separated by filtration (0.45 μm Nylon filter) and oven-dried at 333 K. All the gold-on-carbon catalysts used in reaction were previously treated in order to avoid the adsorption contribution to the overall phenol and TOC uptake and to enable the catalytic activity comparison to the others supported gold catalysts. The pre-treatment consisted of washing the catalyst in a phenol solution at the same operating conditions as the oxidation tests but in absence of hydrogen peroxide during 24 h. Also, adsorption runs were performed with Au/TiO_2 catalyst for each target compound (phenol and benzyl alcohol) in order to study the influence of the nature of the pollutant on the gold reactivity. Additionally, some experiments were performed at a lower stirring rate (200 rpm in an orbital shaker, Julabo, SW22) to confirm the absence of external mass transfer limitations. The particle size employed (d_p < 80 μm) also assures the absence of internal diffusion limitations (Thiele modulus around 3×10^{-3}, based on the observed initial phenol oxidation rate of the Au(3)/C catalyst). The homogenous contribution was assessed by working in absence of catalyst.

0.5 mL-samples were periodically collected by a syringe, and immediately injected in a vial, submerged in crushed ice, containing cold milliQ water. The diluted samples were subsequently filtered and analyzed by different techniques. Phenol, benzyl alcohol and aromatic by-products were identified and quantified by HPLC (Varian Pro-Start 240) and low molecular weight acids by IC with anionic chemical suppression (Metrohm, mod. 761 Compact IC). Detailed operational conditions of these techniques have been reported elsewhere [38]. TOC was measured in a TOC analyzer (Shimadzu TOC V_{SCH}). Hydrogen peroxide concentration was quantified by colorimetric titration using the titanium sulfate method. The efficiency of hydrogen peroxide consumption is given by the ratio of TOC to hydrogen peroxide conversions. A value equal to 1 means the best achievement according to the stoichiometric amount of hydrogen peroxide used in all the experiments. Metal content in the liquid effluents was determined by TXRF (Extra-II Rich & Seifert spectrometer). The presence of hydroxyl radicals was visualized by the methylene blue dye test. Effluents at different reaction times were drop-sampled on a blue methyl tip prepared according to Satoh et al. protocol [39]. The decolorization of the tip corresponds to the oxidation of the methylene blue dye (dark blue colour) to methyl blue radical cation (colourless) by the hydroxyl radicals.

Table 1
Gold loading, particle size and percentage of exposed surface gold species of the catalysts tested and their preparation method.

Catalyst	$[Au]_{total}$ (wt %)	Au_p (nm)	Au^0 fraction (%)	$Au^{\delta+}$ fraction (%)	Au/M[a]	Preparation method
Au/TiO_2	0.80	3.1 ± 1.8	79	21	0.014	Co-precipitation
Au/Fe_2O_3	4.48	3.6 ± 0.9[b]	26	74	0.045	Co-precipitation
Au(3)/C	0.13	5.1 ± 2.0[c]	69	31	0.002	Citrate-capped-gold immobilization
Au(5)/C	0.47	4.9 ± 1.0	72	28	0.004	Tannic acid-capped-gold immobilization
Au(7)/C	0.48	6.8 ± 1.7	71	29	0.025	Tannic acid-capped-gold immobilization
Au(10)/C	0.50	9.1 ± 1.1	69	31	0.015	Tannic acid-capped-gold immobilization

[a] M represents Ti, Fe or C, as corresponds.
[b] Data provided by the supplier, WGC.
[c] Two modes centered at 3.2 and 5.7 nm.

3. Results and discussion

3.1. Catalyst characterization

Table 1 summarizes the average gold particle sizes obtained from TEM. Some representative micrographs and the particle size distributions can be seen in Fig. 1. The commercial catalysts, Au/TiO_2 and Au/Fe_2O_3, contain spherical particles of around 3 nm. With respect to the gold-on-carbon catalysts, the spherical morphology and the particle size of the initial colloidal gold were maintained after immobilization on the activated carbon with the exception of the 3 nm citrate-capped gold particles (Table 1). In this case, a bimodal distribution, centered at 3.2 and 5.7 nm was found which leads to an average particle size of 5.1 ± 2.0 nm. This

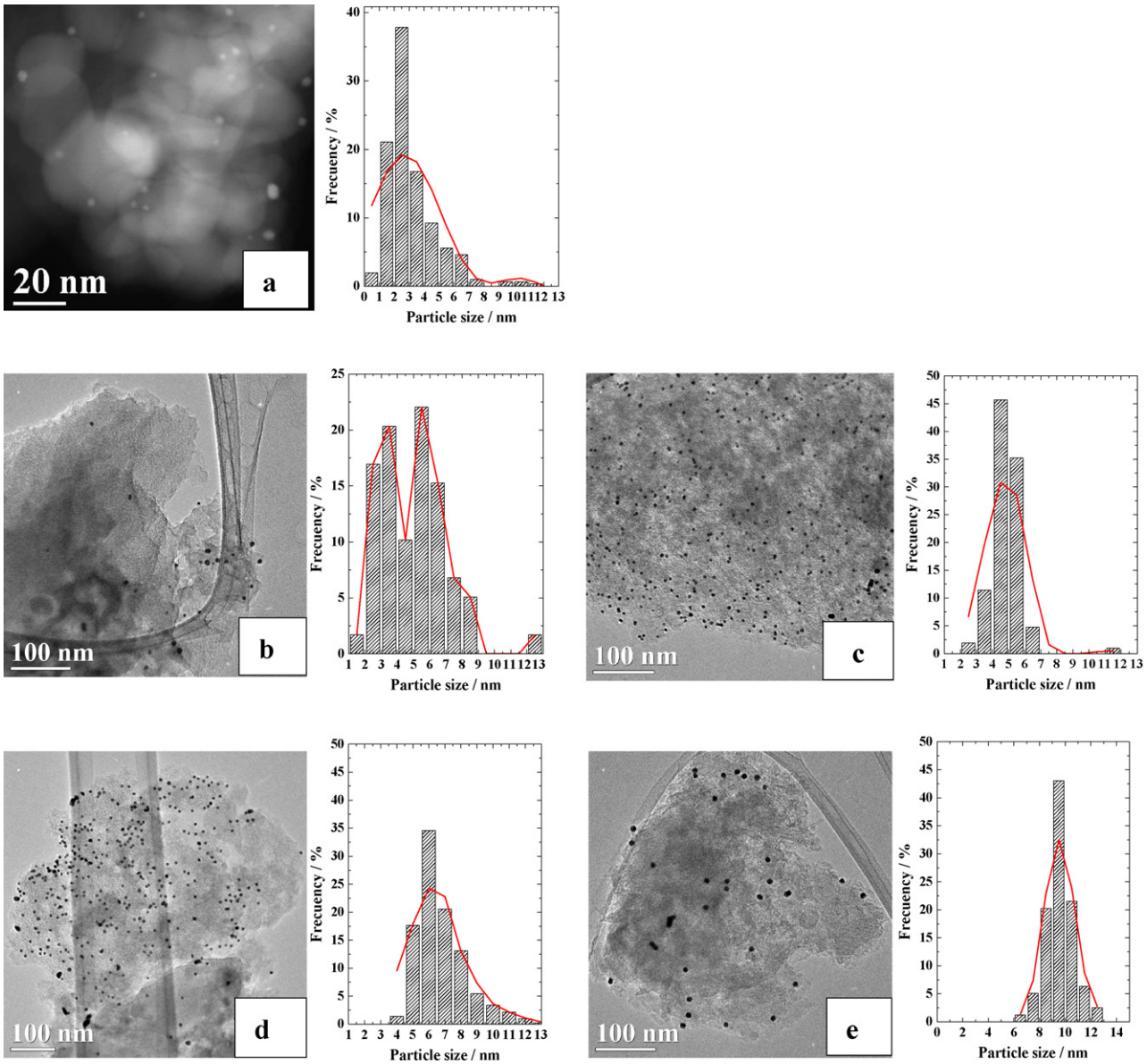

Fig. 1. HAADF-STEM (a) and TEM micrographs and particle size distributions corresponding to 0.8 wt.% Au/TiO_2 (a), 0.13 wt.% Au(3)/C (b), 0.5 wt.% Au(5)/C (c), 0.5 wt.% Au(7)/C (d), 0.5 wt.% Au(10)/C samples (e).

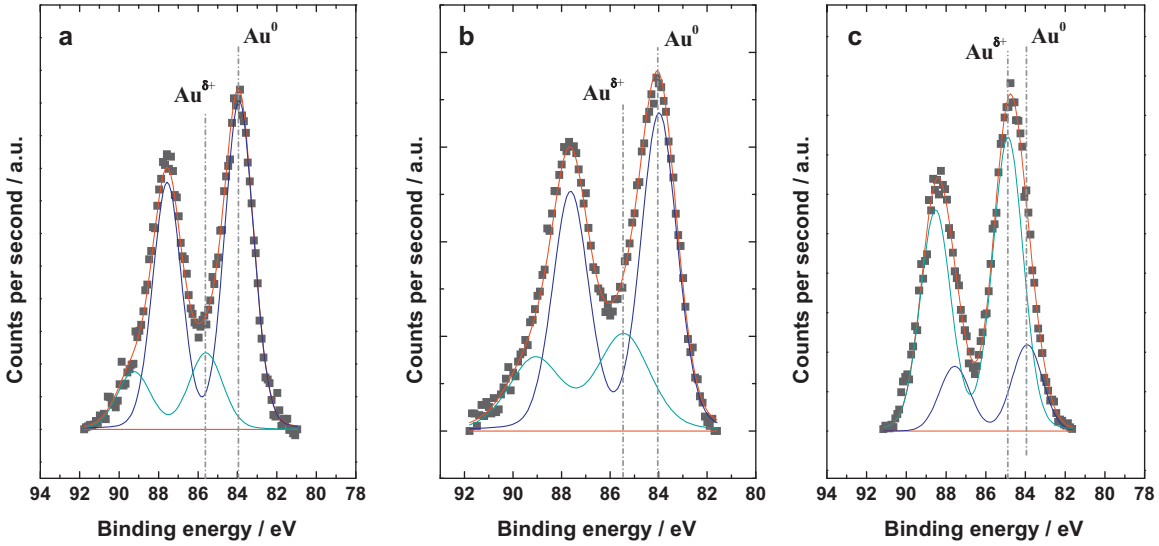

Fig. 2. Au 4f core level of XPS spectra of the Au/TiO_2 (a), Au(3)/C (b) and Au/Fe_2O_3 catalysts.

Au(3)/C is the gold-on-carbon catalysts containing the highest proportion of smaller gold particles and it will be selected for studying the effect of the nature of the support (TiO_2, Fe_2O_3 and C). The gold contents measured by ICP are also summarized in Table 1. The targeted 0.5 wt% was confirmed in the tannic acid-immobilized gold catalysts (Au(5)/C, Au(7)/C and Au(10)/C). However, citrate-immobilized gold catalyst (Au(3)/C), yielded only 0.13 wt% gold. This different behavior can be ascribed to the nature of the capping agent, in particular, the molecular structure and acid/basic properties. Regarding the structure, sodium citrate ($NaC_6H_7O_7$) as well as tannic acid ($C_{76}H_{52}O_{46}$) contain oxygen, which is the heteroatom bound to gold. However, different particle architecture is expected. Citrate anion is a small molecule adsorbed on the gold surface forming a self-assembled layer [40] whereas tannic acid is a rigid polymer conforming a gold core-porous shell that provides a better stability of the particle during the immobilization process and can guarantee the particle size conservation. Regarding the acid/basic properties, capping agents induce the pH of the colloidal gold sols that will affect the adsorption capacity of the carbon. The citrate gold sol has a pH of 8 and the carbon a pH at the point of zero charge of 7, therefore, the carbon surface is negatively charged and will repel the citrate anions. Then, the fade of the red colour of the sol during the preparation of this catalyst was caused by the preferential gold coating on the beaker surface, as confirmed by the ICP analysis of the wash-out of the beaker with aqua regia. In contrast, the acidic pH of the tannic acid-capped gold sols facilitates the adsorption of tannic acid on the carbon surface allowing a successful uptake of the targeted load for these series of catalysts.

Gold speciation, elemental composition in atom percent (at.%) and relative gold abundance (Au/M ratio, M being Ti, Fe or C, as corresponding) at the surface of the investigated catalysts, as obtained from the XPS analyzes, are also collected in Table 1. XPS spectra of the Au 4f core level and the binding energies of Au $4f_{7/2}$ photoelectrons can be seen in Fig. 2 and in Table S1 (Supporting Information), respectively. Au^0 and $Au^{\delta+}$ species were detected in all the catalysts. The binding energy of Au $4f_{7/2}$ photoelectrons in Au/TiO_2 and Au/C indicates that gold is present mainly as Au^0 (84.0 eV). A second gold species is observed at higher binding energies (85.5 eV) corresponding to electro-deficient gold ($Au^{\delta+}$). However, in the case of Au/Fe_2O_3, $Au^{\delta+}$ is the main exposed species. Therefore, the $Au^{\delta+}/Au^0$ surface ratio seems to be more dependent of the nature of the support than of the particle size. According to the Au/M ratio, gold is specially exposed in Au/Fe_2O_3.

3.2. Activity experiments

3.2.1. Support effect

The activity of gold nanoparticles can be strongly affected by the support, as observed with other gold-catalyzed processes [41–43]. To study this fact in the wet hydrogen peroxide oxidation, the catalytic activity of small gold particles, with an average particle size of around 3 nm, immobilized on different supports (TiO_2, C and Fe_2O_3), was studied. The results with phenol, after 4 h reaction time, are summarized in Fig. 3. As can be seen, hydrogen peroxide decomposition is promoted in presence of gold catalyst whereas the oxidation and mineralization of phenol is not always accordingly achieved. Au(3)/C and Au/Fe_2O_3 are active catalysts but Au/TiO_2 shows a moderate oxidation activity in spite of promoting a faster decomposition of hydrogen peroxide than Au(3)/C. The methylene blue test provided clear proof of the lower concentration of hydroxyl radicals in the liquid phase with Au/TiO_2 than with Au(3)/C (see Fig. S1 in the Supplementary information). Therefore, hydroxyl radicals produced in presence of Au/TiO_2 catalyst are mainly consumed in parasite reactions, yielding, for instance,

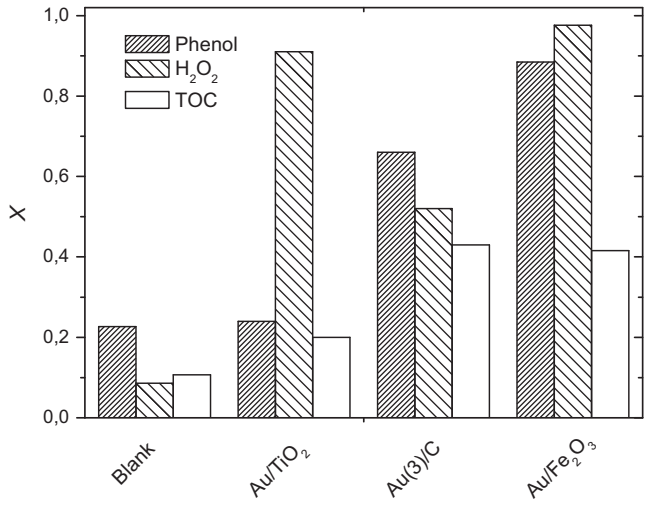

Fig. 3. Conversions achieved upon wet peroxide oxidation with gold nanoparticles on different supports after 4 h of reaction (C^0_{phenol} = 4.5 g/L, $C^0_{H_2O_2}$ = 22.5 g/L, C_{CAT} = 2.5 g/L, T = 353 K, p = 1 atm, pH_0 3.5).

Table 2
Initial rates and TOFs for hydrogen peroxide decomposition, phenol oxidation and mineralization.

Catalyst	r_o ($g_i/g_{solid}/h$)			$TOF_o \times 10^{-4}$ (h^{-1})		
	H_2O_2	Phenol	TOC	H_2O_2	Phenol	TOC
C	1.8	0.5	1.0	–	–	–
Au/TiO_2	17.0	1.3	1.0	2.52	0.07	0.07
Au(3)/C	13.5	2.7	2.0	16.70	1.19	1.08
Au(5)/C	10.3	2.2	1.5	4.07	0.32	0.25
Au(7)/C	4.4	1.4	1.1	2.27	0.25	0.25
Au(10)/C	2.9	2.0	1.5	1.87	0.47	0.43

Initial rates calculated as $(r_o)_i = (-dC_i/dt)_o \times 1/C_{CAT}$; TOFs (mol substrate/mol exposed gold/h). Mol exposed gold calculated assuming spherical nanoparticles and according to the particle size distribution derived by TEM.

oxygen and water, on the gold surface [35], instead of being released to the liquid phase where they could react with phenol molecules.

Leaching of gold was negligible (in the order of 0.01% of the initial gold load) whereas a significant concentration of iron was measured in the liquid phase from the experiments with the Au/Fe_2O_3 catalyst (73% of the initial iron was leached after 24 h of reaction). Thus, in the case of Au/Fe_2O_3, gold activity is masked by the significant homogeneous contribution caused by the dissolved iron. For this reason, and also considering the unlikely application of this unstable catalyst, Au/Fe_2O_3 was discarded for further studies.

The initial TOF values for hydrogen peroxide decomposition, phenol oxidation and mineralization (TOC) are summarized in Table 2 where the supremacy of Au(3)/C can be seen whereas Au/TiO_2 is by far the least active catalyst for phenol oxidation and mineralization. Noteworthy that in spite of the lower amount of gold particles with sizes equal or lower to 3 nm in Au(3)/C with respect to Au/TiO_2 (Fig. 1), as well as the lower proportion of Au^0 on the surface, the much lower exposition of gold (Au/M ratio values) (Table 1) and the presence of a capping agent (citrate), which may hinder the accessibility of the reactants to the active sites and/or act as catalyst surface poison [44], gold nanoparticles are clearly more active supported on carbon than on TiO_2. Interestingly, activated carbons are not inert supports and they usually exhibit activity in oxidation reactions [45]. Therefore, the Au(3)/C activity may consist on the contribution of both gold nanoparticles and carbon activity. To check this hypothesis, the activity of titania and carbon was explored at the selected operating conditions. The results demonstrated that only carbon (also previously contacted with a phenol solution) was active because hydrogen peroxide was decomposed on its surface and consequently phenol oxidation and mineralization took place. The initial rate values of carbon and Au(3)/C (Table 2) show the much lower activity of the former. The fact that 3 nm gold particles being much more active on carbon than on titania together with the low initial carbon activity suggest a synergistic effect between the gold particles and the carbon support. Considering the excellent adsorption properties of activated carbon, it is indeed tempting to assign this synergism to activated carbon-promoted or enhanced adsorption of phenol on gold nanoparticles. This adsorption of organic molecules on the gold surface can have two consequences: the decrease in the production of hydroxyl radicals by the partial occupation of the active sites by the organics and the increase of reacting chance between hydroxyl radicals and organics, both phenomena in detriment of the useless recombination and scavenging reactions of hydroxyl radicals. In both cases, a better use of the oxidant and high TOF values are obtained. In this sense, the use of supports with some adsorption capacity such as activated carbons and other modified carbonaceous materials is recommended.

According to the above discussion, a reaction mechanism for the oxidation of phenol on the carbon-supported gold nanoparticles has been proposed as shown in Fig. 4, where the following steps are schematized: (i) adsorption of phenol and, preferentially, hydrogen peroxide on the gold-support interface, (ii) production of hydroxyl and hydroperoxyl radicals on the gold surface though some extension also occurs on the carbon surface and (iii) reactions between hydroxyl and phenol molecules on the gold surface. Also, hydroxyl radicals are released to the liquid phase where they react with phenol in solution. Parasite reactions, by the recombination of radicals species present, can take place yielding hydrogen peroxide and also oxygen and water.

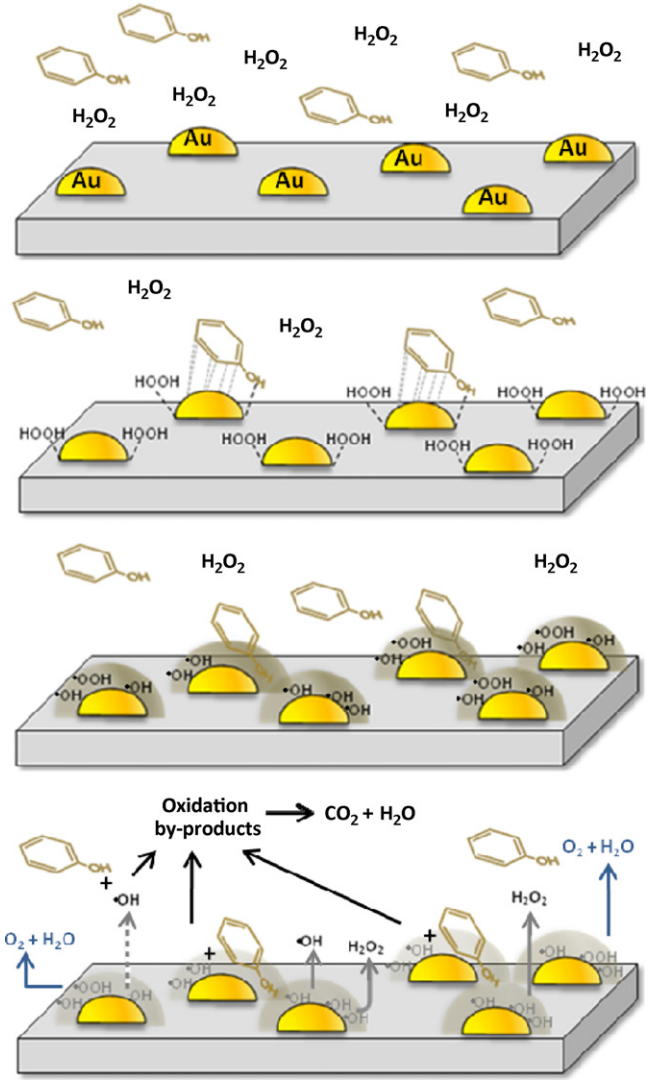

Fig. 4. Proposed mechanisms for phenol wet peroxide oxidation over carbon-supported gold nanoparticles.

3.2.2. Gold particle size effect

The particle size dependence of phenol oxidation was investigated by using gold particles of selected sizes immobilized on carbon, catalysts named Au(3)/C, Au(5)/C, Au(7)/C and Au(10)/C. The results in terms of initial rates and TOFs for hydrogen peroxide decomposition, phenol and TOC disappearance are summarized in Table 2. As a general trend, the lower the particle size the higher the TOF. This is especially evident for the catalytic decomposition of hydrogen peroxide where the highest TOF values are obtained. The size dependence becomes less significant in phenol oxidation and mineralization at gold particle sizes beyond 5 nm. We can anticipate that phenol diffusion hindrance could be expected with tannic acid but not with citrate shields [44], fact that can contribute to the

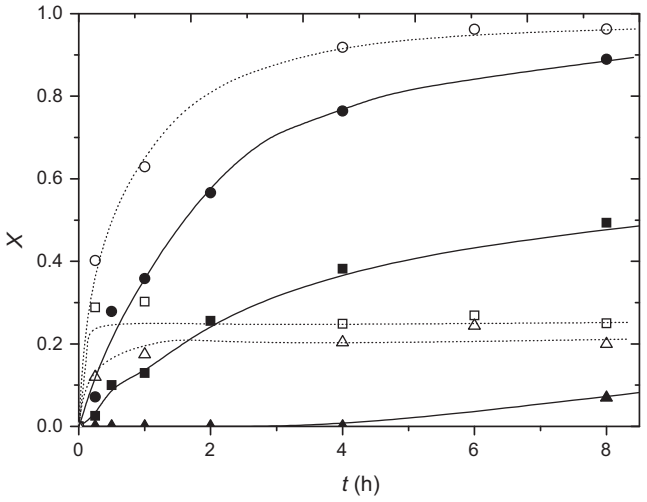

Fig. 5. Hydrogen peroxide (circle), target compound (squares) and TOC (triangles) conversions *vs.* reaction time upon phenol (dot line) and benzyl alcohol (solid line) wet peroxidation over Au/TiO_2 catalysts ($C^0_{pollutant} = 4.5$ g/L, $C^0_{H_2O_2}$ corresponding to the stoichiometric amount for mineralization of the pollutants, $C_{CAT} = 2.5$ g/L, $T = 353$ K, $p = 1$ atm, pH_0 3.5).

supremacy of the Au(3)/C catalyst and to moderate the particle size effect in the tannic acid-capped gold.

3.2.3. *Effect of the target compound*

The low phenol conversions observed with the Au/TiO_2 catalyst are in agreement with the results of Navalon et al. [37]. Interestingly, Ni et al. [46] achieved conversions of 90–99% in the selective oxidation of solvent-free aromatic and aliphatic alcohols with hydrogen peroxide; in that work, phenols were not tested. The low activity of gold in the wet peroxide oxidation of phenol could be ascribed to the nature of this compound. Phenols are less reactive than alcohols in gold–H_2O_2 systems. To understand this aspect, oxidation experiments have been carried out with Au/TiO_2 and benzyl alcohol as target compound. The conversion profiles (hydrogen peroxide, starting compound and TOC) with reaction time are given in Fig. 5. The results obtained with phenol have been also included for the sake of comparison. As observed, hydrogen peroxide is decomposed slowly in presence of benzyl alcohol and the oxidation of this alcohol takes place progressively. Benzyl alcohol is oxidized to aromatic by-products (benzaldehyde and benzoic acid) but mineralization only takes place after an induction period of several hours and reaches fairly low values along the 8 h of the experiment. A quite different scenario can be described for phenol since in this case, the initial oxidation of this compound is faster

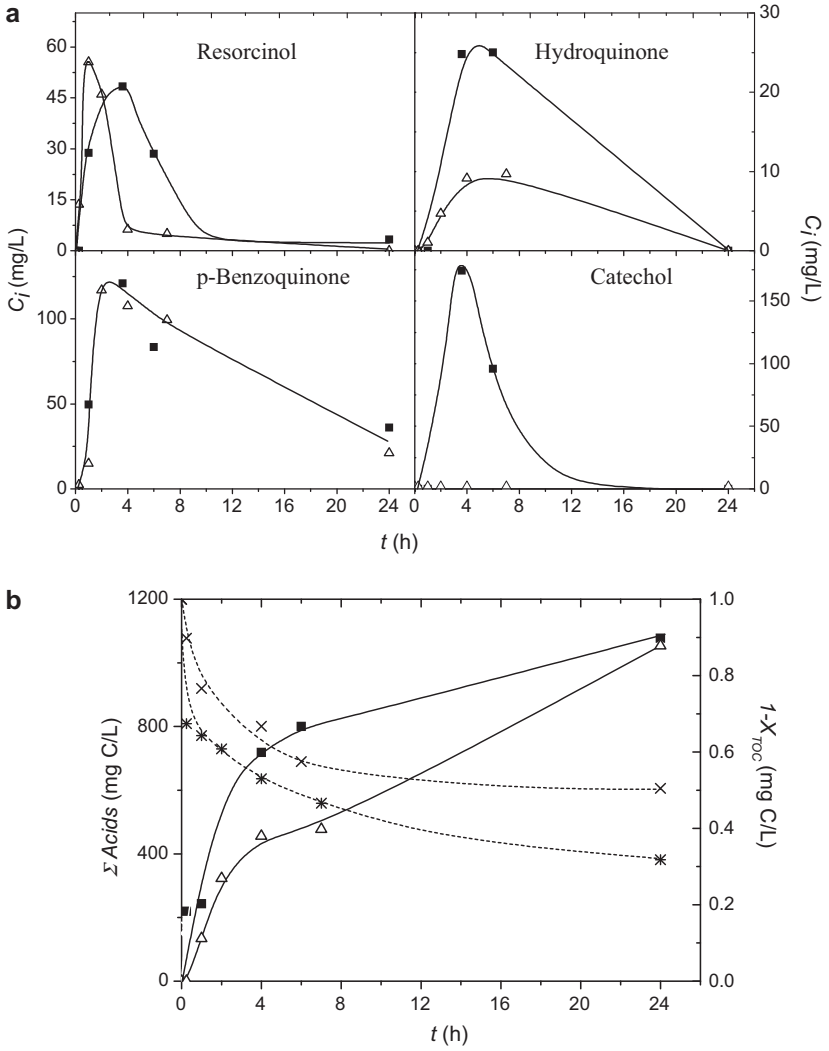

Fig. 6. Evolution of by-products and TOC removal from phenol peroxidation over Au(3)/C (open symbols and *) and bare activated carbon (closed symbols and ×) at the operating conditions of Fig. 3.

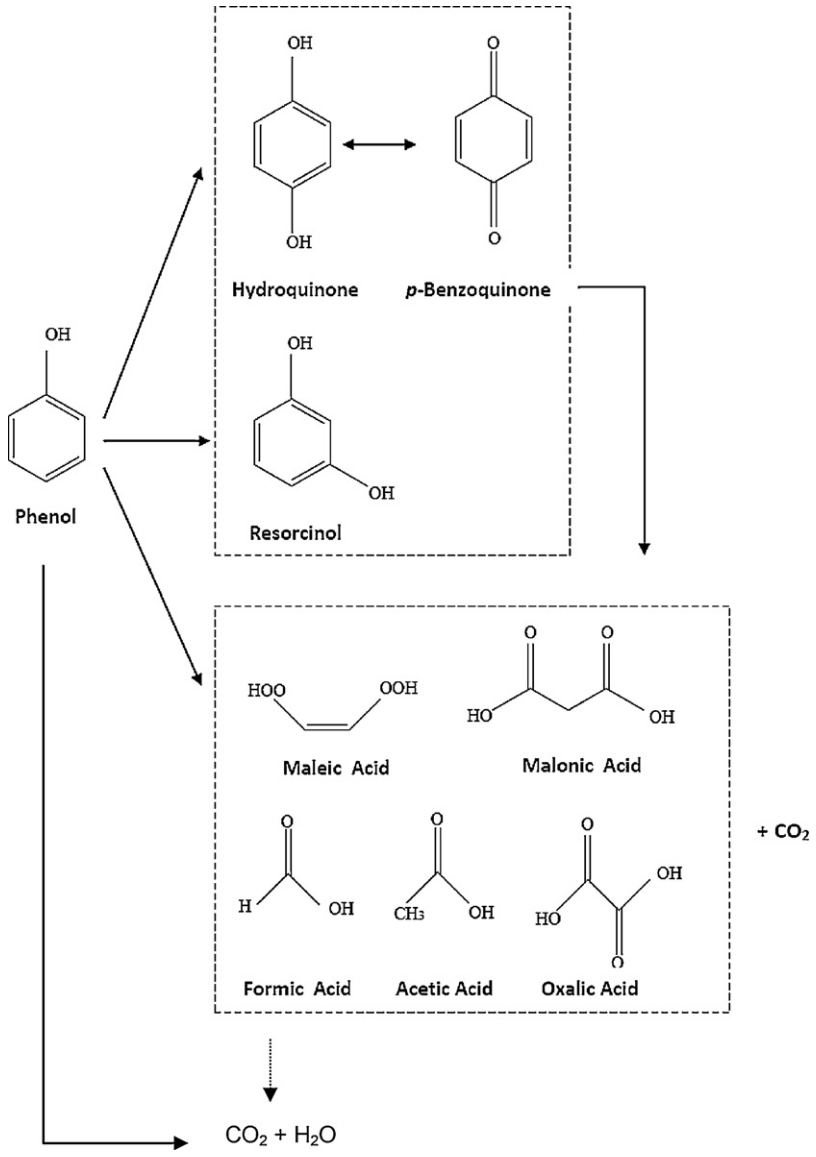

Fig. 7. Reaction pathway for wet peroxidation of phenol over gold on carbon nanoparticles.

than that of the alcohol but it stops after 0.5 h, though hydrogen peroxide is still decomposing on the gold surface. TOC reduction is observed from the beginning of reaction and phenol and TOC conversion curves are close indicating that hydroxyl radicals are consumed from the beginning in the mineralization of by-products from phenol oxidation. These results suggest some differences in the reaction mechanism associated to the oxidation of the two compounds.

For alcohols, it is generally accepted the formation of a gold–alcoholate complex which evolves to more oxidized products, typically to the aldehyde, via β-hydrogen abstraction and without the participation of the oxidant, which eventually will regenerate the active site [47–49]. This mechanism cannot be assumed for phenols because of the absence of the β-hydrogen in the phenol molecule. Electrochemical analysis has been demonstrated covalent adsorption of phenol on gold electrodes by the oxygen atom and weak adsorption by the aromatic ring [50]. We believe that a similar situation can take place in the case of gold nanoparticles. To obtain experimental evidences on the different interaction between the two organic molecules tested and gold, adsorption experiments on gold supported on an inert support, reproducing the operating conditions of the oxidation tests but in absence of hydrogen peroxide were performed for each individual compound.

The results substantially showed higher uptake for benzyl alcohol than phenol (6.2 vs. 1.6 mmol per gram of Au/TiO_2, respectively, after 24 h contact time). Additionally, in the case of benzyl alcohol, benzaldehyde and benzoic acid were progressively detected upon time, remaining below 600 mg/L. These results confirm the reactivity between the alcohol and gold and also show the participation of water since benzoic acid instead of benzaldehyde was the major by-product [51]. In the case of phenol, experiment by-products were never detected in the liquid media and TOC and phenol disappearance were coincident so that only adsorption took place.

Therefore, benzyl alcohol and phenol show a different interaction with gold. We suggest that the kind of affinity of benzyl alcohol towards gold implies a major competition for the active sites that determines a slower decomposition of hydrogen peroxide. This leads to a progressive oxidation of benzyl alcohol and, as the concentration of the by-products increases, also a progressive mineralization (note that the benzyl alcohol by-products, benzaldehyde and benzoic acid, are more refractory to oxidation

than phenol and quinones). In the case of phenol-Au/TiO_2 systems, hydrogen peroxide is submitted to a lower competition for the active sites, which results in a faster hydrogen peroxide decomposition. Then, the radical species yield from this hydrogen peroxide decomposition are accumulated on the gold surface and recombined giving oxygen instead of reacting with phenol in solution. Therefore, the use of organic pollutants with reactivity towards gold, *i.e.* alcohols, results in somehow lower hydrogen peroxide decomposition rates and progressive oxidation and mineralization. It is a similar effect to the observed when a support with adsorption capacity towards the organic pollutant is employed.

3.3. Selectivity of the Au/C catalysts

Complete mineralization of phenol was far from being achieved with any of the gold catalysts tested (Fig. 3). These results are not unexpected attending to the nature of that compound and the mild operating conditions tested. Conversions of phenol were significantly higher than those of TOC, suggesting that relatively important amounts of by-products are produced. The by-products detected in the reaction media were aromatics and low molecular weight carboxylic acids, the latter were responsible of the decreasing pH of the reaction media up to around 2.3 after 24 h of reaction. The time-evolution of the reaction products and TOC removal with the Au(3)/C catalyst is depicted in Fig. 6, which also shows the results obtained with the bare activated carbon. The aromatic by-products identified in presence of gold were resorcinol, hydroquinone and *p*-benzoquinone (Fig. 6a) and the carboxylic acids were maleic, malonic, acetic, oxalic and formic, which have been grouped in Fig. 6b. According to the curve profiles (Fig. 6), the aromatic intermediates are completely converted upon sufficient reaction time to carboxylic acids, of substantially lower ecotoxicity and quite refractory to the oxidation under the conditions tested. Their residual concentration represented around 28% of the initial phenol in terms of carbon. The TOC values calculated from the identified by-products (not shown) were fairly close to the experimental TOC measurements (Fig. 6b) so that the oxidation intermediates are almost completely identified and quantified and condensation by-products, typically formed in Fenton and Fenton-like oxidations of phenol, are not present in the effluent.

The results of Fig. 6 also evidence the influence of gold on the by-product distribution. Resorcinol and hydroquinone were oxidized more rapidly than in the presence of bare carbon, appearing in lower concentrations, whereas catechol was not detected in presence of gold. A similar situation was observed with the different gold-sized-on-carbon catalysts prepared (Au(5)/C, Au(7)/C and Au(10)/C). Therefore, gold allows the hydroxylation of phenol in *meta* and *para* position (responsible for resorcinol and hydroquinone formation, respectively) and inhibits *orto*-hydroxylation (catechol formation). The different orientation of phenol on gold and on carbon surface may explain the different selectivity. Phenol is predominantly attached to gold by the oxygen atom [50] whereas the attachment on carbon occurs by the aromatic ring [52]. Thus, a vertical orientation to the surface and a parallel one are, respectively, expected. In the former, the attack of radicals to the *orto* position can be hindered and then catechol formation inhibited whereas in the latter the accessibility of the *orto* position is similar to the others. In addition to the faster oxidation of the aromatic intermediates, carboxylic acids were also detected in lower amounts than with bare carbon. Considering the refractoriness of the carboxylic acids and the enhanced TOC removal (Fig. 6b), the direct oxidation of phenol to CO_2 and H_2O is considered as a likely path.

The inhibition of the reaction path to catechol, ecotoxic intermediate typically formed in H_2O_2-oxidation of phenol, and the faster oxidation of dyhydroxybenzenes, oxidation hydroquinone being particularly important since it is by far the most ecotoxic intermediate of phenol oxidation route [53,54], together with the enhanced mineralization are important issues proving the beneficial effect of gold catalysts on the process investigated.

The distribution of by-products shown in Fig. 6 corresponds to a parallel–serial reaction network. Phenol is simultaneously oxidized to aromatic intermediates, carboxylic acids and CO_2 in parallel reactions. Subsequently, the aromatic by-products are oxidized to the organic acids of substantially lower ecotoxicity and higher biodegradability. Fig. 7 shows the proposed reaction pathway for the oxidation of phenol over supported gold on carbon nanoparticles.

4. Conclusions

Supported gold nanoparticles for wet peroxide oxidation processes must be designed considering that small particles, preferentially lower than 3 nm, exhibit higher TOF values and that the support can strongly enhance gold activity. The use of supports with high adsorption capacity such as activated carbons, and other modified carbonaceous materials, is preferred for a better use of the oxidant and to improve the TOF values for the oxidation and mineralization. The proposed mechanism for gold-on-carbon catalysts considers the preferential adsorption of the reactants on the gold-support interface, the production of hydroxyl and hydroperoxyl radicals on the gold surface and the reaction between hydroxyl radicals and phenol molecules on the gold surface as well as in the liquid phase. This process is more efficient for organic pollutants with a good affinity towards gold (those forming intermediate complexes *i.e.* alcohols). An important feature regarding the environmental interest of gold nanoparticles refers to catalytic selectivity with enhanced mineralization.

Acknowledgments

The authors thank the Spanish MICINN for the financial support through the projects CTQ2010-14807 and CTQ2008-03988/PPQ. The MINTEK Company is also gratefully acknowledged for the samples of Au/TiO_2 catalyst provided within the project "AuTEK Catalysis R&D".

Appendix A. Supplementary data

Supplementary data associated with this article can be found, in the online version, at doi:10.1016/j.apcatb.2011.09.020.

References

[1] H.J.H. Fenton, J. Chem. Soc. 65 (1894) 899.
[2] A. Goi, M. Trapido, Chemosphere 46 (2002) 913.
[3] S. Esplugas, J. Jiménez, S. Contreras, E. Pascual, M. Rodríguez, Water Res. 36 (2002) 1034.
[4] N. Al-Hayek, J.P. Eymery, M. Dore, Water Res. 19 (1985) 657.
[5] S. Perathoner, G. Centi, Top. Catal. 33 (2005) 207.
[6] C.P. Huang, Y.H. Huang, Appl. Catal. A: Gen. 346 (2008) 140.
[7] N. Al-Hayek, M. Doré, Water Res. 24 (1990) 973.
[8] P. Bautista, A.F. Mohedano, N. Menendez, J.A. Casas, J.J. Rodríguez, 2nd European Conference on Environmental Applications of Advanced Oxidation Processes, Cyprus September 8–11, 2009.
[9] K. Hanna, T. Kone, G. Medjahdi, Catal. Commun. 9 (2008) 955.
[10] C.P. Huang, Y.F. Huang, H.P. Cheng, Y.H. Huang, Catal. Commun. 10 (2009) 561.
[11] F. Martínez, J.A. Melero, J.A. Botas, M.I. Pariente, R. Molina, Ind. Eng. Chem. Res. 46 (2007) 4396.
[12] G. Calleja, J.A. Melero, F. Martínez, R. Molina, Water Res. 39 (2005) 1741.
[13] J.A. Melero, G. Calleja, F. Martínez, R. Molina, M.I. Pariente, Chem. Eng. J. 131 (2007) 245.
[14] N. Crowther, F. Larachi, Appl. Catal. B: Environ. 46 (2003) 293.
[15] N. Gokulakrishnan, A. Pandurangan, P.K. Sinha, Ind. Eng. Chem. Res. 48 (2009) 1556.
[16] J. Barrault, M. Abdellaoui, C. Bouchoule, A. Majesté, J.M. Tatibouët, A. Louloudi, N. Papayannakos, N.H. Gangas, Appl. Catal. B: Environ. 27 (2000) 225.

[17] J.G. Carriazo, E. Guélou, J. Barrault, J.M. Tatibouët, S. Moreno, Appl. Clay Sci. 22 (2003) 303.
[18] E. Guélou, J. Barrault, J. Fournier, J.M. Tatibouët, Appl. Catal. B: Environ. 44 (2003) 1.
[19] J. Guo, M. Al-Dahhan, Ind. Eng. Chem. Res. 42 (2003) 2450.
[20] C.B. Molina, J.A. Casas, J.A. Zazo, J.J. Rodríguez, Chem. Eng. J. 118 (2006) 29.
[21] K. Fajerwerg, J. Foussard, A. Perrard, H. Debellefontaine, Water Sci. Technol. 35 (1997) 103.
[22] G. Centi, S. Perathoner, T. Torre, M.G. Verduna, Catal. Today 55 (2000) 61.
[23] O.P. Petsunova, G.L. Elizarova, Z.R. Ismagilov, M.A. Kerzhentsev, V.N. Parmon, Catal. Today 75 (2002) 219.
[24] E.V. Kuznetsova, E.N. Savinov, L.A. Vostrikova, V.N. Parmon, Appl. Catal. B: Environ. 51 (2004) 165.
[25] O.A. Makhotkina, S.V. Preis, E.V. Parkhomchuk, Appl. Catal. B: Environ. 84 (2008) 821.
[26] S.G. Huling, R.G. Arnold, R.A. Sierka, P.K. Jones, D.D. Fine, J. Environ. Eng. 126 (2000) 595.
[27] J.A. Zazo, J.A. Casas, A.F. Mohedano, J.J. Rodríguez, Appl. Catal. B: Environ. 65 (2006) 261.
[28] A. Quintanilla, A.F. Fraile, J.A. Casas, J.J. Rodríguez, J. Hazard. Mater. 146 (2007) 582.
[29] C.S. Castro, M.C. Gerreiro, L.C.A. Oliveira, M. Goncalves, A.S. Anastasio, M. Nazzarro, Appl. Catal. A: Gen. 367 (2009) 53.
[30] J.H. Ramírez, F.J. Maldonado-Hódar, A.F. Pérez-Cadenas, C. Moreno-Castilla, C.A. Costa, L.M. Madeira, Appl. Catal. B Environ. 75 (2007) 312.
[31] F. Duarte, F.J. Maldonado-Hódar, A.F. Pérez-Cadenas, L.M. Madeira, Appl. Catal. B: Environ. 85 (2009) 139.
[32] Q. Liao, J. Sun, L. Gao, Colloids Surf. A: Physicochem. Eng. Aspects 345 (2009) 95.
[33] A. Rey, M. Faraldos, A. Bahamonde, J.A. Casas, J.A. Zazo, J.J. Rodríguez, Ind. Eng. Chem. Res. 47 (2008) 8166.
[34] Y.F. Han, N. Phonthammachai, K. Ramesh, Z. Zhong, T. White, Environ. Sci. Technol. 42 (2008) 908.
[35] A. Quintanilla, C.M. Domínguez, S. Blasco, J.A. Casas, J.J. Rodríguez, 2nd European Conference on Environmental Applications of Advanced Oxidation Processes, Cyprus September 8–11, 2009.
[36] R. Martín, S. Navalon, M. Alvaro, H. Garcia, Appl. Catal. B: Environ. 103 (2011) 246.
[37] S. Navalon, R. Martin, M. Alvaro, H. Garcia, Angew. Chem. Int. Ed. 49 (2010) 840.
[38] A. Quintanilla, J.A. Casas, J.A. Zazo, A.F. Mohedano, J.J. Rodriguez, Appl. Catal. B: Environ. 62 (2006) 115.
[39] A.Y. Satoh, J.E. Trosko, S.J. Masten, Environ. Sci. Technol. 41 (2007) 2881.
[40] Y. Yang, S. Matsubara, M. Nogami, J. Shi, W. Huang, Nanotechnology 17 (2006) 2821.
[41] M. Haruta, Catal. Today 36 (1997) 153.
[42] M. Haruta, M. Daté, Appl. Catal. A: Gen. 222 (2001) 427.
[43] A. Grirrane, A. Corma, H. Garcia, Science 322 (2008) 1661.
[44] A. Quintanilla, V.C.L. Butselaar-Orthlieb, C. Kwakernaak, W.G. Sloof, M.T. Kreutzer, F.J. Kapteijn, Catalysis 271 (2010) 104.
[45] F. Stuber, J. Font, A. Fortuny, C. Bengoa, A. Eftaxias, A. Fabregat, Top. Catal. 33 (2005) 3.
[46] J. Ni, W.J. Yu, L. He, H. Sun, Y. Cao, H.Y. He, K.N. Fan, Green Chem. 11 (2009) 756.
[47] T. Mallat, A. Baiker, Chem. Rev. 104 (2004) 3037.
[48] A. Abad, A. Corma, H. Garcia, Chem. Eur. J. 14 (2008) 212.
[49] G. Brink, I.W.C.E. Arends, R.A. Sheldon, Science 287 (2000) 1636.
[50] R.0. Lezna, N.R. de Tacconi, S.A. Centeno, A.J. Arvia, Langmuir 7 (1991) 1241.
[51] W.B. Hou, N.A. Dehm, R.W.J. Scott, J. Catal. 253 (2008) 22.
[52] J.M. Valente Nabais, J.A. Gomes, P.J.M. Suhas, C. Carrott, S. Laginhas, J. Roman, Hazard. Mater. 167 (2009) 904.
[53] A. Santos, P. Yustos, A. Quintanilla, F. García-Ochoa, J.A. Casas, J.J. Rodriguez, Environ. Sci. Technol. 38 (2004) 133.
[54] J.A. Zazo, J.A. Casas, C.B. Molina, A. Quintanilla, J.J. Rodríguez, Environ. Sci. Technol. 41 (2007) 7164.